

A Journal of the Gesellschaft Deutscher Chemiker

Angewandte Chemie

GDCh

International Edition

www.angewandte.org

Accepted Article

Title: Generation of Tunable Ultrastrong White-Light Emission by Activation of a Solid Supramolecule through Bromonaphthylpyridinium Polymerization

Authors: Yu-Yang Hu, Xian-Yin Dai, Xiaoyun Dong, Man Huo, and Yu Liu

This manuscript has been accepted after peer review and appears as an Accepted Article online prior to editing, proofing, and formal publication of the final Version of Record (VoR). The VoR will be published online in Early View as soon as possible and may be different to this Accepted Article as a result of editing. Readers should obtain the VoR from the journal website shown below when it is published to ensure accuracy of information. The authors are responsible for the content of this Accepted Article.

To be cited as: *Angew. Chem. Int. Ed.* **2022**, e202213097

Link to VoR: <https://doi.org/10.1002/anie.202213097>

RESEARCH ARTICLE

Generation of Tunable Ultrastrong White-Light Emission by Activation of a Solid Supramolecule through Bromonaphthylpyridinium Polymerization

Yu-Yang Hu⁺,^[a] Xian-Yin Dai⁺,^[a] Xiaoyun Dong,^[a] Man Huo,^[a] and Yu Liu^{*[a]}

[a] Dr. Y.-Y. Hu, X.-Y. Dai, X. Dong, M. Huo, Prof. Dr. Yu Liu
College of Chemistry
State Key Laboratory of Elemento-Organic Chemistry
Nankai University, Tianjin 300071, P. R. China
E-mail: yuliu@nankai.edu.cn

[+] These authors contributed equally to this work.

Abstract: Herein, we reported solid supramolecular bromonaphthylpyridinium polymers (P-BrNp), which exhibited tunable phosphorescence emission enabled by sulfobutylether- β -cyclodextrin (SBE- β -CD) and diarylethene derivative in amorphous state. The monomer BrNp gave single fluorescence emission at 490 nm, while an apparent RTP at 550 nm emerged for P-BrNp copolymers with various feed ratios. Benefiting from the fluorescence-phosphorescence dual emission property, P-BrNp-0.1 displayed an ultrahigh white-light emission quantum yield of 83.9%. Moreover, the subsequent assembly with SBE- β -CD further enhanced phosphorescent quantum yield of P-BrNp-0.1 from 64.1% up to 71.3%, accompanied by the conversion of photoluminescence emission from white to yellow. Notably, diarylethene monomers as photoswitch were also introduced into above supramolecules to realize the reversible RTP emission, which can be competently applied in switchable data encryption and multifunctional writing ink.

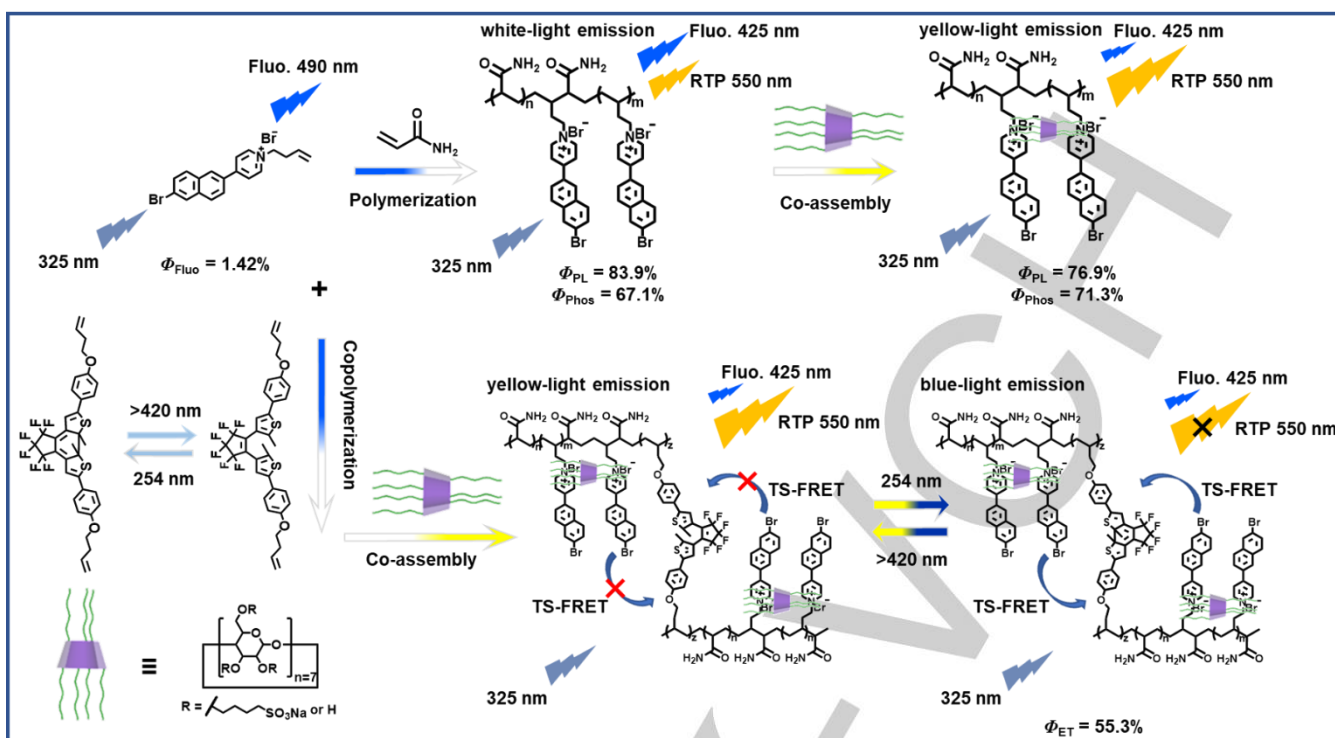
Introduction

Tunable luminescent supramolecular materials that respond to external stimuli such as humidity,^[1] temperature,^[2] mechanical force,^[3] and light,^[4] have received extensive attention in recent years due to their potential application in the fields of biological imaging,^[5] invisible Ink,^[6] and optoelectronic devices.^[7] However, the current reported stimulus-responsive luminescent supramolecular materials mainly depended on fluorescence, which impeded their further applications due to the inherent nanosecond-scale lifetimes.^[8] To this end, purely organic room-temperature phosphorescence (RTP) is considered as an alternative benefiting from its unique properties like long lifetime and large Stokes shift.^[9] However, realizing RTP-based materials with highly efficient emission still remain enormous challenges because of the weak spin-orbit coupling efficiency, molecular vibration and oxygen microenvironment-mediated nonradiative

quenching of the triplet states.^[10] Therefore, numerous methods have recently been adopted to induce organic RTP including crystallization,^[11] polymer matrix,^[12] host-guest interaction,^[13] and doping.^[14] Moreover, the synergistic strategy by incorporating multiple interactions has also proved to be an effective approach to achieve efficient phosphorescence performance. For example, we reported the copolymer of bromophenyl pyridinium complexing with cucurbit[n]uril ($n = 6-8$) synergistically realizing RTP emission with ultralong lifetime and high phosphorescence quantum yield.^[15] In addition, Dexter electron exchange and cluster excitons strategy were also utilized to construct ultralong phosphorescent materials with high efficiency.^[16]

More recently, phosphorescence resonance energy transfer systems have gradually become a new research hotspot in virtue of their multicolor luminescent output,^[17] showing broad application prospects in the fields of biological imaging^[18] and information security.^[19] Meanwhile, among various external stimuli, light control with clean, non-invasive, and remote-controlling features is of particular interest.^[20] Therefore, the integration of light-responsive building blocks into RTP-based energy transfer process is a novel strategy to construct multicolor photoluminescence materials. For instance, Xu et al. constructed a photoreversible fluorescence and RTP switching by integrating phosphor dibenzofuran with photoswitch dithienylbenzothiophene.^[21] Ma et al. reported radiative energy transfer system between a RTP material and fluorescence dyes achieving tunable persistent luminescent materials.^[22] We also reported supramolecular pseudopolyrotaxanes of two luminophores modified polyethylene glycol derivatives which can co-assembled with α -cyclodextrin excellently realizing excitation-wavelength-responsive and time-dependent multicolor materials.^[23] However, the construction of responsive RTP materials in a noninvasive controlled manner concurrently accompanied by multicolor conversions and ultrahigh emission quantum yield is still rare.

RESEARCH ARTICLE



Scheme 1. Schematic illustration of the construction of tunable ultrastrong white-light emission by activation of a solid supramolecule through bromonaphthylpyridinium polymerization.

Here, we constructed a series of amorphous naphthylpyridinium-acrylamide copolymers (P-BrNp) with various feed ratios (from 0.001% to 1%) via copolymerization strategy, in which P-BrNp-0.1 exhibited ultrahigh white-light emission quantum yield 83.9% with fluorescence-phosphorescence dual emission at room temperature. Notably, such a copolymer displayed an enhanced phosphorescence quantum yield up to 71.3% after further complexation with sulfolbutylether- β -cyclodextrin (SBE- β -CD) under ambient conditions. Furthermore, diarylethene monomers serving as photoswitch were also introduced into above binary supramolecular systems to realize reversible RTP emission through an efficient phosphorescence resonance energy transfer with phosphorescence quenching efficiency as 55.3% (Scheme 1). Significantly, these fabricated supramolecular systems can be competently applied in stimuli-responsive data encryption and anti-counterfeiting, which offer a new insight for the construction of more advanced stimuli-responsive RTP supramolecular materials.

Results and Discussion

Bromonaphthyl-butenylpyridinium (BrNp) was synthesized according to the routes shown in Scheme S1, Supporting Information and fully characterized by ^1H NMR, ^{13}C NMR spectroscopies and HR-MS (Figure S1-S3). BrNp copolymerized with acrylamide to form binary copolymer according to the routes (Scheme S2). The gel permeation chromatography (GPC) analysis was first performed to confirm the formation of copolymers (Figure S7-S10), in which the copolymers with high molecular weight showed better phosphorescence emission performance (Figure S11). The observed ratio of comonomers was determined by the concentration-absorbance standard curve of BrNp solution at 325 nm (Figure S12 and Table S1). Then the

excitation and absorption spectra of these copolymers were measured in solid state, which exhibited almost the same peak shape with a peak of 325 nm due to the same BrNp chromophore (Figure S13-S14). The monomer showed single emission at 490 nm in the photoluminescence (PL) spectrum with the lifetime as 1.34 ns and with fluorescence quantum yield of 1.4% (Figure S15). In contrast, the P-BrNp-0.1 displayed dual emission at 425 nm and 550 nm in the PL spectrum, while only one emission peak at 550 nm was observed in the time-gated spectrum (delay time = 0.1 ms) (Figure 1a and 1b), preliminarily proving that the peak at 425 nm was a short-lived emission, and the peak at 550 nm was a long-lived emission. Subsequently, the lifetimes at 425 nm and 550 nm were measured, where the lifetime at 425 nm was 4.64 ns while the lifetime at 550 nm was 10.19 ms (Figure 2c and Figure S16b), which confirmed that the polymer exhibited dual emission of fluorescence ($\lambda_{\text{max}} = 425$ nm) and phosphorescence ($\lambda_{\text{max}} = 550$ nm). The large Stokes shift (225 nm) of these copolymers further illustrated that the delayed luminescence is phosphorescence but not delayed fluorescence (Figure 1c). It was noted that these copolymers all exhibited broad phosphorescence peaks centered on 550 nm which may be due to the solvation effect from polar acrylamide polymer media on the phosphor. Notably, the P-BrNp-0.1 especially realized white-light emission as depicted by the CIE 1931 chromaticity diagram (Figure 1d) where the CIE coordinates was located at (0.33, 0.37), and this white-light emission was consistent with naked eye observation under the excitation of UV 365 nm (Figure S17).

The ratio of phosphors has great influence on the phosphorescence intensity and lifetimes of polymers.^[15] In order to obtain the polymer possessing stronger emission and longer lifetime, we synthesized copolymers containing different ratio of phosphors (1%, 0.1%, 0.01%, 0.001% and named P-BrNp-1, P-BrNp-0.1, P-BrNp-0.01, P-BrNp-0.001, respectively). The PL spectra, phosphorescence emission spectra and time-resolved

RESEARCH ARTICLE

PL decay curves of these polymers were shown in Figure 1a-b, Figure S16 and S18. The P-BrNp-0.1 had the strongest PL and phosphorescence intensity, and nearly 15 times stronger than P-BrNp-0.001. And the P-BrNp-0.01 had the highest phosphorescence lifetime at 550 nm up to 10.31 ms (9.40 ms for P-BrNp-1, 10.19 ms for P-BrNp-0.1 and 9.41 ms for P-BrNp-0.001). Surprisingly, regardless of the proportion of phosphor mixed in, the polymer always showed white-light emission as depicted by the CIE 1931 chromaticity diagram (Figure 1d), and we could observe white light under portable UV lamp (Figure S17). Significantly, P-BrNp-1 was closest to pure white light, and the CIE coordinates was calculated at (0.33, 0.34). Therefore, the simple copolymerization can greatly promote the phosphorescence by suppressing the molecular vibrations, rotations, promoting ISC, and shielding quenchers.^[12a] Due to P-BrNp possessed heavy atoms which are universal introduced to facilitate intersystem crossing (ISC), P-BrNp had higher phosphorescence intensity and phosphorescence quantum yield, but heavy atoms will accelerate radiative and nonradiative decay rates of the triplet excited state, so P-BrNp only had millisecond phosphorescent lifetime.^[24] White-light quantum yields (PL quantum yields) and phosphorescence quantum yields of these polymers were measured (Figure S19-S26). Consistent with the PL intensity, P-BrNp-0.1 had the highest white-light quantum yield up to 83.9% which contained fluorescence quantum yield 19.8% and phosphorescence quantum yield 64.1%. Considering P-BrNp-0.1 possessed highest white-light quantum yield (83.9%) and higher lifetime (10.19 ms), we chose P-BrNp-0.1 as a mode to further study. In addition, the X-ray powder diffraction (XRD) was used to explore the microstructure of these binary copolymers, which showed that they were all amorphous states (Figure S27a).

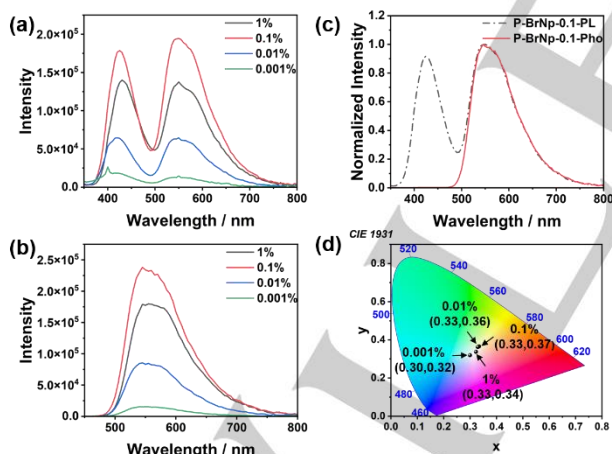


Figure 1. (a) PL spectra ($\lambda_{\text{ex}} = 325$ nm) of P-BrNp containing different ratio of phosphors (1% to 0.001%) in the solid state. (b) Phosphorescence emission spectra ($\lambda_{\text{ex}} = 325$ nm, delay time = 0.1 ms) of P-BrNp containing different ratio of phosphors (1% to 0.001%) in the solid state. (c) PL and phosphorescence emission spectra of P-BrNp-0.1 (Normalized spectra). (d) The CIE 1931 chromaticity diagram of P-BrNp containing different ratio of phosphors (1% to 0.001%) in the solid state.

On account of multicharged cyclodextrin based on positively/negatively charged can interact with oppositely charged polymers to achieve effective encapsulation and aggregation,^[25]

we chose SBE- β -CD to construct supramolecular assembly with P-BrNp-0.1. For the purpose of achieving the best phosphorescence properties by addition of SBE- β -CD, we tried adding different ratios of SBE- β -CD into P-BrNp-0.1 (the mass ratio of P-BrNp-0.1 and SBE- β -CD (M_R) from 1:1 to 1:10). The PL spectra and phosphorescence emission spectra showed that the M_R at 1:3 had the strongest phosphorescence intensity (Figure S28). The different ratio of SBE- β -CD could also change the phosphorescence lifetime at 550 nm of P-BrNp-0.1, and the M_R at 1:1 had the longest lifetime up to 10.72 ms (Figure S29). Due to the M_R at 1:3 possessed the strongest phosphorescence intensity, we chose this ratio for follow-up experiments. When SBE- β -CD was added to P-BrNp-0.1 for grinding, the P-BrNp-0.1@SBE- β -CD showed dual emission in the PL spectrum (Figure 2a). The original fluorescence peak at 425 nm decreased and blue-shifted to 400 nm, and the original phosphorescence peak at 550 nm enhanced. The phosphorescence spectrum (delay time = 0.1 ms) of P-BrNp-0.1@SBE- β -CD also showed a single peak at 550 nm, and 1.7 times stronger than P-BrNp-0.1 (Figure 2b). Next, the time-resolved PL decay curves of P-BrNp-0.1@SBE- β -CD was measured (Figure 2c). The phosphorescence lifetime of P-BrNp-0.1@SBE- β -CD at 550 nm reached 10.58 ms, longer than P-BrNp-0.1 (10.19 ms); and the fluorescence lifetime of P-BrNp-0.1@SBE- β -CD at 420 nm was 3.11 ns (Figure S30), shorter than P-BrNp-0.1 (4.64 ns). Compared with P-BrNp-0.1, the PL quantum yield of P-BrNp-0.1@SBE- β -CD showed a slight decrease from 83.9% to 76.9%, whereas the phosphorescence quantum yield increased from 67.1% to 71.3% (Figure S31-S32). According to the standard methods, the intersystem crossing rate constants (k_{isc}) could be calculated based on the measured lifetimes and quantum yields of P-BrNp-0.1 and P-BrNp-0.1@SBE- β -CD, where the k_{isc} of P-BrNp-0.1@SBE- β -CD were $3.04 \times 10^8 \text{ S}^{-1}$ which was higher than that of P-BrNp-0.1 ($1.73 \times 10^8 \text{ S}^{-1}$), thereby resulting in the higher phosphorescent quantum yield of P-BrNp-0.1@SBE- β -CD (Table S2). The supramolecular assembly with SBE- β -CD can not only immobilize the phosphorescent molecular motion to suppress the vibrational dissipation but also provided a protective environment for phosphors,^[13a] thereby further effectively promoting phosphorescence emission. Significantly, due to a decrease in fluorescence at 425 nm and an increase in phosphorescence at 550 nm after P-BrNp-0.1 addition of SBE- β -CD, the original white-light of P-BrNp-0.1 changed to yellow-light of P-BrNp-0.1@SBE- β -CD under portable UV lamp (Figure S33). The CIE diagram in Figure 2d also showed that it moved from the white-light area (0.33,0.37) to the yellow-light area (0.38,0.47). Therefore, tunable luminescent materials from white to yellow could be realized via the co-assembly process between P-BrNp and SBE- β -CD. Like P-BrNp-0.1, the XRD results showed that the P-BrNp-0.1@SBE- β -CD was also amorphous states (Figure S27a). In addition, the luminescence properties (e.g. PL spectra, phosphorescence emission spectra and phosphorescence lifetime) of the solid powder obtained by freeze-drying the polymer with SBE- β -CD in water and the solid powder obtained by directly grinding were also measured, which showed no obvious differences between them (Figure S34).

RESEARCH ARTICLE

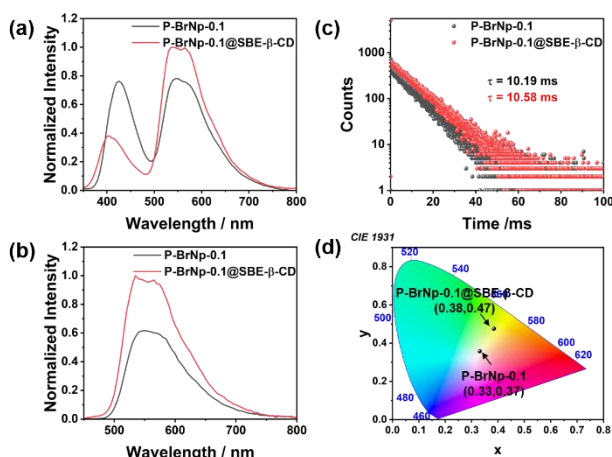


Figure 2. (a) PL spectra ($\lambda_{\text{ex}} = 325$ nm) of P-BrNp-0.1 (black) and P-BrNp-0.1@SBE- β -CD (red) in the solid state. (b) Phosphorescence emission spectra ($\lambda_{\text{ex}} = 325$ nm, delay time = 0.1 ms) of P-BrNp-0.1 (black) and P-BrNp-0.1@SBE- β -CD (red) in the solid state. (c) Time-resolved PL decay curves of P-BrNp-0.1 (black) and P-BrNp-0.1@SBE- β -CD (red) in the solid state. (d) The CIE 1931 chromaticity diagram of P-BrNp-0.1 and P-BrNp-0.1@SBE- β -CD. ($M_{\text{R}} = 1:3$).

In order to gain more insights of mechanism of enhanced phosphorescence performance, the UV titration experiment was first performed to prove that there was an interaction between BrNp and SBE- β -CD, revealing that the absorption peak at 325 nm gradually decreased and appeared blue shift (Figure S35a). Similarly, the UV titration experiment between P-BrNp and SBE- β -CD also showed similar results (Figure S35b). Furthermore, to verify whether BrNp was included into the cavity of SBE- β -CD, we performed 1D/2D NMR experiments, which indicated that the proton signals of BrNp presented no significant chemical shifts in the presence of SBE- β -CD and there were no obvious correlation peaks between BrNp and SBE- β -CD (Figure S36-S38). Similarly, circular dichroism spectroscopy (CD) showed that the BrNp with SBE- β -CD did not exhibit any Cotton effect in CD spectrum (Figure S39). The above experiments demonstrated that the BrNp did not encapsulated into the cavity of SBE- β -CD, so we speculated that the system mainly existed the electrostatic interaction between BrNp (positive charge) and SBE- β -CD (negative charge). In control experiments, sodium 1-butanedisulfonate and parent β -CD were added to P-BrNp-0.1 to study their influence on the phosphorescence performance of P-BrNp-0.1, respectively. It was found that their phosphorescence spectra at 550 nm (delay time = 0.1 ms) were not significantly different from those of the previous polymer alone (Figure S40). On the contrary, the phosphorescence intensity of P-BrNp-0.1@SBE- β -CD had significant improvement compared to P-BrNp-0.1. Moreover, hyaluronic acid (HA) with negative charges also co-assembled with P-BrNp-0.1, where the PL and phosphorescence intensity of P-BrNp-0.1@HA were weaker than original P-BrNp-0.1 (Figure S41). These control experiments jointly indicated that the unique torus-shaped cyclic conformation and edge sodium 1-butanedisulfonate groups of SBE- β -CD play important roles in the improvement of the RTP behavior.

Diarylethylene (DAE) and its derivatives possessing excellent light-responsive photoisomerization properties, were often used to singlet-to-singlet Förster resonance energy transfer (SS-FRET).^[26] However, there are few reports on triplet-to-singlet

Förster resonance energy transfer (TS-FRET) based on DAE. Hence, a new diarylethene derivative (DAE-ene) was also synthesized according to the routes shown in Scheme S3, and fully characterized by ^1H NMR, ^{13}C NMR spectroscopies and HR-MS (Figure S4-S6). Through ^1H NMR spectroscopies, it was proved that the synthetic DAE-ene had excellent photoisomerization properties. As shown in Figure S42, the protons on the diarylethylene skeleton of o-DAE-ene showed different chemical shift changes with the prolongation of 254 nm UV irradiation time. When irradiated with 254 nm UV for 180 minutes, the DAE-ene reached a photostable state, and the ring-closing conversion rate for the transformation from o-DAE-ene to c-DAE-ene was approximately determined as 95% by the ^1H NMR integral of the final product after UV illumination. More interestingly, a complete recovery of the ^1H NMR spectra o-DAE-ene was observed when c-DAE-ene was irradiated with visible light (>420 nm, 5 min), indicating that DAE-ene could achieve reversible switching between open-ring and closed-ring (Figure S43). Subsequently, the P-DAE-ene was synthesized (Scheme S4) and the photoisomerization property of P-DAE-ene was showed by UV-vis spectra. As shown in Figure S44, P-o-DAE-ene had an absorption at 297 nm. When irradiated with 254 nm UV, P-o-DAE-ene gradually transformed into the closed form (P-c-DAE-ene) with the appearance of a new peak at 600 nm and the decrease of the peak at 297 nm. Moreover, the subsequent irradiation with visible light could achieve the conversion of closed form P-c-DAE-ene into the open form P-o-DAE-ene. Notably, the absorption peak of P-c-DAE-ene had obvious spectral overlap with the phosphorescence emission peak of the P-BrNp-0.1 (Figure S45), thus it was chosen as the acceptor to build the TS-FRET system. Next, the ternary polymer (P-BrNp-0.1-DAE-1) was synthesized, which was composed of BrNp, DAE-ene and acrylamide (Scheme S5). Subsequently, the photo-controlled phosphorescence properties of P-BrNp-0.1-DAE-1 was investigated under 254 nm UV irradiation. As shown in Figure 3a, when irradiated with 254 nm UV, P-BrNp-0.1-DAE-1 underwent the photoisomerization process with the decrease of the peak centered at 550 nm, and reached equilibrium in nearly 3 minutes. With the irradiation of 254 nm UV, the o-DAE-ene in P-BrNp-0.1-DAE-1 gradually changed into the closed form (c-DAE-ene), so the triplet energy of BrNp was transferred to the singlet energy of c-DAE-ene. Due to the quenching of the phosphorescence peak at 550 nm, the color of P-BrNp-0.1-DAE-1 changed from origin white to blue (Figure 3a, inset). With the increase of UV irradiation time, the phosphorescence lifetime of P-BrNp-0.1-DAE-1 at 550 nm has been reduced from the original 8.94 ms to final 4.21 ms (Figure 3c). In control experiment, P-DAE-ene itself did not have fluorescence and phosphorescence emission (Figure S46).

RESEARCH ARTICLE

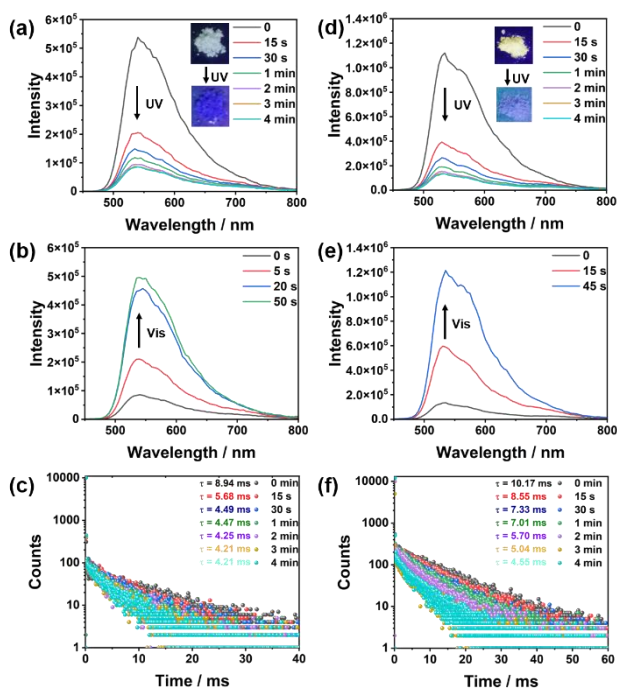


Figure 3. (a) Phosphorescence emission spectra ($\lambda_{\text{ex}} = 325$ nm, delay time = 0.1 ms) of P-BrNp-0.1-DAE-1 upon irradiation with 254 nm UV in the solid state. (b) Phosphorescence emission spectra ($\lambda_{\text{ex}} = 325$ nm, delay time = 0.1 ms) of P-BrNp-0.1-DAE-1 upon irradiation with visible light (>420 nm) in the solid state. (c) Time-resolved PL decay curves of P-BrNp-0.1-DAE-1 at 550 nm after different UV light irradiation time in the solid state. (d) Phosphorescence emission spectra ($\lambda_{\text{ex}} = 325$ nm, delay time = 0.1 ms) of P-BrNp-0.1-DAE-1@SBE- β -CD upon irradiation with 254 nm UV in the solid state. (e) Phosphorescence emission spectra ($\lambda_{\text{ex}} = 325$ nm, delay time = 0.1 ms) of P-BrNp-0.1-DAE-1@SBE- β -CD upon irradiation with visible light (>420 nm) in the solid state. (f) Time-resolved PL decay curves of P-BrNp-0.1-DAE-1@SBE- β -CD at 550 nm after different UV light irradiation time in the solid state.

In this system, the value of phosphorescence quenching efficiency calculated by the change of lifetime was up to 52.9%. Subsequently, the P-BrNp-0.1-DAE-1 was exposed with visible light (>420 nm), and the c-DAE-ene gradually turned into the open form, so the TS-FRET was cut off and the original phosphorescence peak of the P-BrNp gradually recovered (Figure 3b). Moreover, the phosphorescence lifetime of P-BrNp-0.1-DAE-1 at 550 nm can almost return to the initial level when continuously irradiated with visible light (Figure S47a). The reversible TS-FRET process could be achieved by the transitions of o-DAE-ene and c-DAE-ene. In addition, SBE- β -CD was also added to P-BrNp-0.1-DAE-1 for grinding (mass ratio of P-BrNp-0.1-DAE-1 and SBE- β -CD = 1:3), P-BrNp-0.1-DAE-1@SBE- β -CD also showed yellow light under portable UV lamp (Figure 3d, inset), which was the same properties as P-BrNp-0.1@SBE- β -CD. When irradiated with 254 nm UV, P-BrNp-0.1-DAE-1@SBE- β -CD also underwent the photoisomerization process with the decrease of the peak centered at 550 nm (Figure 3d). Unlike previous P-BrNp-0.1-DAE-1, it could process from origin yellow to blue (Figure 3d, inset). The continuous UV irradiation resulted in the gradual reduction of phosphorescence lifetime of P-BrNp-0.1-DAE-1@SBE- β -CD at 550 nm from the original 10.17 ms to final 4.55 ms (Figure 3f). The value of phosphorescence quenching efficiency was calculated as 55.3%, which was higher than P-BrNp-0.1-DAE-1 (52.9%), which was probably ascribed that TS-FRET could be facilitated by the SBE- β -CD. Similarly, both

phosphorescence emission intensity and lifetime of P-BrNp-0.1@SBE- β -CD at 550 nm can be nearly restored to the original state by continuous irradiation of visible light (Figure 3e and Figure S47b). In the same way, P-BrNp-0.1-DAE-1@SBE- β -CD could realize reversible TS-FRET through 254 nm UV and visible light (>420 nm). In addition, these reversible TS-FRET systems could repeat for several cycles in both phosphorescence emission intensity and lifetime without production of significant light fatigue (Figure S48-S50). In order to study the effect of the amount of DAE-ene on the system, P-BrNp-0.1-DAE-0.5 was synthesized. P-BrNp-0.1-DAE-0.5 could also realize reversible TS-FRET through 254 nm UV and visible light (Figure S51). However, phosphorescence quenching efficiency of P-BrNp-0.1-DAE-0.5 ($\Phi_{\text{P-BrNp-0.1-DAE-0.5}} = 33.4\%$) and P-BrNp-0.1-DAE-0.5@SBE- β -CD ($\Phi_{\text{P-BrNp-0.1-DAE-0.5@SBE-}\beta\text{-CD}} = 37.4\%$) were worse than P-BrNp-0.1-DAE-1 ($\Phi_{\text{P-BrNp-0.1-DAE-1}} = 52.9\%$) and P-BrNp-0.1-DAE-1@SBE- β -CD ($\Phi_{\text{P-BrNp-0.1-DAE-1@SBE-}\beta\text{-CD}} = 55.3\%$), respectively. Additionally, the fluorescence lifetimes of P-BrNp-0.1-DAE-1 and P-BrNp-0.1-DAE-1@SBE- β -CD at 425 nm decreased from 4.10 ns and 4.88 ns to 3.82 ns and 4.57 ns, respectively, which proved the existence of the singlet-singlet FRET process (Figure S52). The attenuation of phosphorescence lifetime under continuous 254 nm UV irradiation and its gradual recovery when exposed to visible light indicated that the above process was a non-radiative energy transfer process benefiting from the photoisomerization of DAE units, and also confirmed that the above process was a TS-FRET process.^[27] Finally, the possible mechanism for this reversible TS-FRET is shown in Figure 4a. The XRD results also showed that the P-BrNp-DAE and P-BrNp-DAE@SBE- β -CD was also amorphous states (Figure S27b).

Owing to the excellent photoswitchable luminescence behaviors and multicolor tunable properties, we successfully applied these supramolecular systems in white light-emitting diode, stimulus-responsive phosphorescent ink and information encryption. The P-BrNp-0.1 was coated onto the surface commercially available diode (excited at 365 nm) which constructed a white light-emitting diode. As shown in Figure 4b, the diode emitted bright white light when the diode is powered from a coin cell battery. In addition, stimulus-responsive phosphorescent ink can realize by dissolving P-BrNp-0.1 or P-BrNp-0.1@SBE- β -CD in water. The characters "NKU" above was written by P-BrNp-0.1% and the "NKU" below was written by P-BrNp-0.1@SBE- β -CD. These characters emitted blue fluorescence under the excitation of 365 nm UV when they were just written. The "NKU" above emitted white light and the "NKU" below emitted yellow light upon exposure to the UV light at 365 nm when these characters dried in oven (Figure 4c). Similarly, when the ambient humidity gradually increases, these characters gradually turn blue. Moreover, the powder of P-BrNp-0.1 and P-BrNp-0.1-DAE-1 were pressed into the shape of a pill, and put on the filter paper as the number "88". The number "88" emitted white light under the excitation of 365 nm UV. However, when irradiating with 254 nm UV lamp, the number "88" became number "11" (blue light) and number "33" (white light). And these numbers recovered number "88" with white light under irradiated by visible light (> 420 nm) (Figure 4d).

RESEARCH ARTICLE

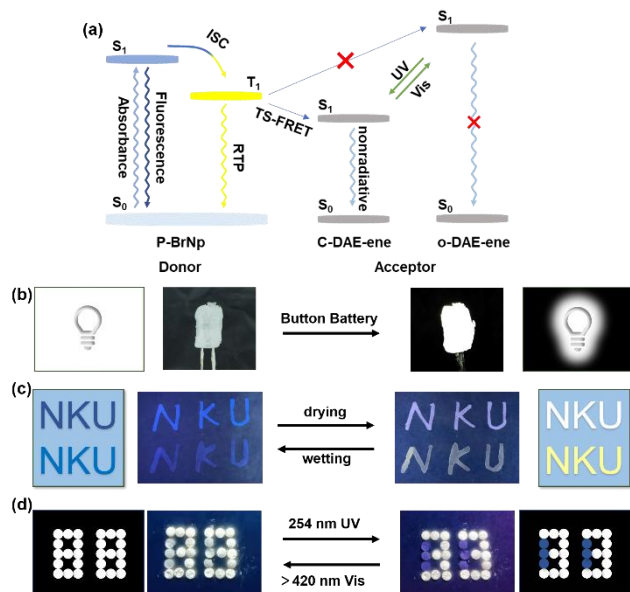


Figure 4. (a) Simplified Jablonski diagram to explain the possible mechanism for reversible TS-FRET process in the present case. (b) Photographs of white light-emitting diode (P-BrNp-0.1 fixed with polymethyl methacrylate onto the surface of diode). (c) Photographs of stimulus-responsive phosphorescent ink. (d) Photographs of digit encryption.

Conclusion

In summary, we successfully fabricated a type of organic room-temperature phosphorescence (RTP) materials activated by bromonaphthylpyridinium polymerization, which showed stimuli-responsive capacities enabled by diarylethylene (DAE) and sulfobutylether- β -cyclodextrin (SBE- β -CD). Due to the copolymerization with acrylamide, naphthylpyridinium-acrylamide copolymers (P-BrNp) with fluorescence–phosphorescence dual emission properties realized ultrastrong white-light emission at room temperature, in which the white-light quantum yield of P-BrNp-0.1 reached up to 83.9%. Moreover, the P-BrNp-0.1 could further assemble with SBE- β -CD to promote RTP emission by the synergetic effects of the unique torus-shaped cyclic conformation of SBE- β -CD and the electrostatic interaction, thereby achieving the ultrahigh phosphorescent quantum yield (71.3%) with lifetime of 10.58 ms. In addition, diarylethene monomers were also introduced into above binary supramolecular systems to realize reversible RTP emission with phosphorescence energy transfer efficiency of 55.3%. Significantly, the excellent RTP performance and reversible triplet-to-singlet Förster resonance energy transfer (TS-FRET) process could construct smart organic RTP materials responding to humidity and light stimulation. We believe that this work will provide new ideas for the construction of the stimulus-responsive multicolor materials and have potential applications for white light-emitting diode, humidity sensor and data encryption.

Acknowledgements

This work was financially supported by the National Natural Science Foundation of China (22131008).

Keywords: Bromonaphthylpyridinium • Polymerization • Phosphorescence • White-Light Emission • Sulfobutylether- β -Cyclodextrin

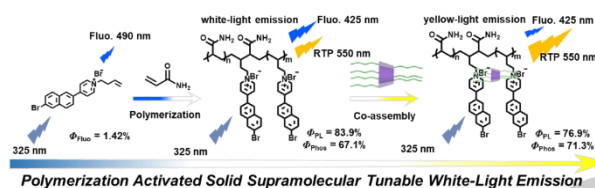
- (a) D. Li, Y. Yang, J. Yang, M. Fang, B. Z. Tang, Z. Li, *Nat. Commun.* **2022**, *13*, 347; (b) D. Li, J. Yang, M. M. Fang, B. Z. Tang, Z. Li, *Sci. Adv.* **2022**, *8*, eabl8392; (c) J. J. Li, H. Y. Zhang, Y. Zhang, W. L. Zhou, Y. Liu, *Adv. Opt. Mater.* **2019**, *7*, 1900589.
- (a) Z. Yu, H. K. Bisoyi, X. M. Chen, Z. Z. Nie, M. Wang, H. Yang, Q. Li, *Angew. Chem. Int. Ed.* **2022**, *61*, e202200466; (b) Z. Xie, X. Zhang, H. Wang, C. Huang, H. Sun, M. Dong, L. Ji, Z. An, T. Yu, W. Huang, *Nat. Commun.* **2021**, *12*, 3522; (c) J. Yang, M. Fang, Z. Li, *InfoMat* **2020**, *2*, 791-806.
- (a) Z. Mao, Z. Yang, Y. Mu, Y. Zhang, Y. F. Wang, Z. Chi, C. C. Lo, S. Liu, A. Lien, J. Xu, *Angew. Chem. Int. Ed.* **2015**, *54*, 6270-6273; (b) H. Wu, P. Zhao, X. Li, W. Chen, H. Agren, Q. Zhang, L. Zhu, *ACS Appl. Mater. Interfaces* **2017**, *9*, 3865-3872.
- (a) X. M. Chen, W. J. Feng, H. K. Bisoyi, S. Zhang, X. Chen, H. Yang, Q. Li, *Nat. Commun.* **2022**, *13*, 3216; (b) J. Yang, J. I. Song, Q. Song, J. Y. Rho, E. D. H. Mansfield, S. C. L. Hall, M. Sambrook, F. Huang, S. Perrier, *Angew. Chem. Int. Ed.* **2020**, *59*, 8860-8863; (c) J. Zhang, Q. Zou, H. Tian, *Adv. Mater.* **2013**, *25*, 378-399; (d) X. Ma, H. Tian, *Acc. Chem. Res.* **2014**, *47*, 1971-1981.
- (a) Y. Fan, S. Liu, M. Wu, L. Xiao, Y. Fan, M. Han, K. Chang, Y. Zhang, X. Zhen, Q. Li, Z. Li, *Adv. Mater.* **2022**, *34*, 2201280; (b) M. L. Yu, W. L. Zhao, F. Ni, Q. Zhao, C. L. Yang, *Advanced Optical Materials* **2022**, *10*, 2102437; (c) X. Y. Dai, Y. Y. Hu, Y. Sun, M. Huo, X. Dong, Y. Liu, *Adv. Sci.* **2022**, *9*, 2200524.
- (a) H. Ju, C. N. Zhu, H. Wang, Z. A. Page, Z. L. Wu, J. L. Sessler, F. Huang, *Adv. Mater.* **2022**, *34*, 2108163; (b) H. Wu, Y. Chen, Y. Liu, *Adv. Mater.* **2017**, *29*, 1605271; (c) Z. Li, X. Liu, G. Wang, B. Li, H. Chen, H. Li, Y. Zhao, *Nat. Commun.* **2021**, *12*, 1363.
- (a) H. Wang, C. N. Zhu, H. Zeng, X. Ji, T. Xie, X. Yan, Z. L. Wu, F. Huang, *Adv. Mater.* **2019**, *31*, 1807328; (b) H. Y. Zhou, D. W. Zhang, M. Li, C. F. Chen, *Angew. Chem. Int. Ed.* **2022**, *61*, e202117872; (c) F. Corsini, A. Nitti, E. Tattsi, G. Mattioli, C. Botta, D. Pasini, G. Griffini, *Adv. Opt. Mater.* **2021**, *9*, 2100182.
- J. Yang, M. Fang, Z. Li, *Acc. Mater. Res.* **2021**, *2*, 644-654.
- (a) J. Guo, C. Yang, Y. Zhao, *Acc. Chem. Res.* **2022**, *55*, 1160-1170; (b) X. Ma, J. Wang, H. Tian, *Acc. Chem. Res.* **2019**, *52*, 738-748; (c) G. Zhang, G. M. Palmer, M. W. Dewhurst, C. L. Fraser, *Nat. Mater.* **2009**, *8*, 747-751; (d) X. Chen, C. Xu, T. Wang, C. Zhou, J. Du, Z. Wang, H. Xu, T. Xie, G. Bi, J. Jiang, X. Zhang, J. N. Demas, C. O. Trindle, Y. Luo, G. Zhang, *Angew. Chem. Int. Ed.* **2016**, *55*, 9872-9876.
- (a) T. Zhang, X. Ma, H. Wu, L. Zhu, Y. Zhao, H. Tian, *Angew. Chem. Int. Ed.* **2020**, *59*, 11206-11216; (b) H. G. Nie, Z. Wei, X. L. Ni, Y. Liu, *Chem. Rev.* **2022**, *122*, 9032-9077.
- (a) M. Singh, K. Liu, S. Qu, H. Ma, H. Shi, Z. An, W. Huang, *Adv. Opt. Mater.* **2021**, *9*, 2002197; (b) H. Zhu, I. Badia-Dominguez, B. Shi, Q. Li, P. Wei, H. Xing, M. C. Ruiz Delgado, F. Huang, *J. Am. Chem. Soc.* **2021**, *143*, 2164-2169; (c) A. Nitti, C. Botta, A. Forni, E. Cariati, E. Lucenti, D. Pasini, *CrystEngComm* **2020**, *22*, 7782-7785.
- (a) N. Gan, H. Shi, Z. An, W. Huang, *Adv. Funct. Mater.* **2018**, *28*, 1802657; (b) H. Gao, X. Ma, *Aggregate* **2021**, *2*, 38; (c) D. Lee, O. Bolton, B. C. Kim, J. H. Youk, S. Takayama, J. Kim, *J. Am. Chem. Soc.* **2013**, *135*, 6325-6329; (d) Y. Su, S. Z. F. Phua, Y. B. Li, X. J. Zhou, D. Jana, G. F. Liu, W. Q. Lim, W. K. Ong, C. L. Yang, Y. L. Zhao, *Sci. Adv.* **2018**, *4*, eaas9732; (e) X. Zhang, T. Xie, M. Cui, L. Yang, X. Sun, J. Jiang, G. Zhang, *ACS Appl. Mater. Interfaces* **2014**, *6*, 2279-2284.
- (a) D. Li, F. Lu, J. Wang, W. Hu, X. M. Cao, X. Ma, H. Tian, *J. Am. Chem. Soc.* **2018**, *140*, 1916-1923; (b) Z. Y. Zhang, Y. Chen, Y. Liu, *Angew. Chem. Int. Ed.* **2019**, *58*, 6028-6032.
- (a) R. Gao, M. S. Kodaimati, D. Yan, *Chem. Soc. Rev.* **2021**, *50*, 5564-5589; (b) B. B. Ding, L. W. Ma, Z. Z. Huang, X. Ma, H. Tian, *Sci. Adv.* **2021**, *7*, eabf9668; (c) K. C. Chong, C. Chen, C. Zhou, X. Chen, D. Ma, G. C. Bazan, Z. Chi, B. Liu, *Adv. Mater.* **2022**, DOI: 10.1002/adma.202201569.

RESEARCH ARTICLE

- [15] Z. Y. Zhang, W. W. Xu, W. S. Xu, J. Niu, X. H. Sun, Y. Liu, *Angew. Chem. Int. Ed.* **2020**, *59*, 18748-18754.
- [16] (a) X. Zhang, L. Du, W. Zhao, Z. Zhao, Y. Xiong, X. He, P. F. Gao, P. Alam, C. Wang, Z. Li, J. Leng, J. Liu, C. Zhou, J. W. Y. Lam, D. L. Phillips, G. Zhang, B. Z. Tang, *Nat. Commun.* **2019**, *10*, 5161; (b) X. Zhang, J. Liu, B. Chen, X. He, X. Li, P. Wei, P. F. Gao, G. Zhang, J. W. Y. Lam, B. Z. Tang, *Matter* **2022**, DOI: 10.1016/j.matt.2022.07.010; (c) G. Li, D. Jiang, G. Shan, W. Song, J. Tong, D. Kang, B. Hou, Y. Mu, K. Shao, Y. Geng, X. Wang, Z. Su, *Angew. Chem. Int. Ed.* **2022**, DOI: 10.1002/anie.202113425.
- [17] (a) S. Garain, B. C. Garain, M. Eswaramoorthy, S. K. Pati, S. J. George, *Angew. Chem. Int. Ed.* **2021**, *60*, 19720-19724; (b) Y. Zhao, L. Ma, Z. Huang, J. Zhang, I. Willner, X. Ma, H. Tian, *Adv. Opt. Mater.* **2022**, *10*, 2102701; (c) S. Kuila, S. J. George, *Angew. Chem. Int. Ed.* **2020**, *59*, 9393-9397; (d) M. Huo, X. Y. Dai, Y. Liu, *Adv. Sci.* **2022**, 2201523.
- [18] (a) Q. Dang, Y. Jiang, J. Wang, J. Wang, Q. Zhang, M. Zhang, S. Luo, Y. Xie, K. Pu, Q. Li, Z. Li, *Adv. Mater.* **2020**, *32*, 2006752; (b) Y. C. Liang, Q. Cao, K. K. Liu, X. Y. Peng, L. Z. Sui, S. P. Wang, S. Y. Song, X. Y. Wu, W. B. Zhao, Y. Deng, Q. Lou, L. Dong, C. X. Shan, *ACS Nano* **2021**, *15*, 16242-16254; (c) M. Huo, X. Y. Dai, Y. Liu, *Angew. Chem. Int. Ed.* **2021**, *60*, 27171-27177; (d) F. Lin, H. Wang, Y. Cao, R. Yu, G. Liang, H. Huang, Y. Mu, Z. Yang, Z. Chi, *Adv. Mater.* **2022**, *34*, 2108333.
- [19] (a) R. Gao, D. Yan, *Chem. Sci.* **2017**, *8*, 590-599; (b) B. Zhou, D. Yan, *Adv. Funct. Mater.* **2019**, *29*, 1807599; (c) W. W. Xu, Y. Chen, Y. L. Lu, Y. X. Qin, H. Zhang, X. Xu, Y. Liu, *Angew. Chem. Int. Ed.* **2022**, *61*, e202115265; (d) Z. Wang, A. Li, Z. Zhao, T. Zhu, Q. Zhang, Y. Zhang, Y. Tan, W. Z. Yuan, *Adv. Mater.* **2022**, DOI: 10.1002/adma.202202182.
- [20] X. Y. Yao, T. Li, J. Wang, X. Ma, H. Tian, *Adv. Opt. Mater.* **2016**, *4*, 1322-1349.
- [21] X. Wang, G. Pan, H. Ren, J. Li, B. Xu, W. Tian, *Angew. Chem. Int. Ed.* **2022**, *61*, e202114264.
- [22] L. Ma, Q. Xu, S. Sun, B. Ding, Z. Huang, X. Ma, H. Tian, *Angew. Chem. Int. Ed.* **2022**, *61*, e202115748.
- [23] Y. Zhang, C. Zhang, Y. Chen, J. Yu, L. Chen, H. Zhang, X. Xu, Y. Liu, *Adv. Opt. Mater.* **2022**, *10*, 2102169.
- [24] X. Ma, C. Xu, J. Wang, H. Tian, *Angew. Chem. Int. Ed.* **2018**, *57*, 10854-10858.
- [25] Z. X. Liu, Y. Liu, *Chem. Soc. Rev.* **2022**, *51*, 4786-4827.
- [26] (a) H. B. Cheng, S. Zhang, E. Bai, X. Cao, J. Wang, J. Qi, J. Liu, J. Zhao, L. Zhang, J. Yoon, *Adv. Mater.* **2022**, *34*, 2108289; (b) L. W. Ma, S. Wang, C. P. Li, D. R. Cao, T. Li, X. Ma, *Chem. Commun.* **2018**, *54*, 2405-2408; (c) X. Dai, X. Dong, Z. Liu, G. Liu, Y. Liu, *Biomacromolecules* **2020**, *21*, 5369-5379.
- [27] (a) A. Kirch, M. Gmelch, S. Reineke, *J. Phys. Chem. Lett.* **2019**, *10*, 310-315; (b) S. Kuila, S. Garain, S. Bandi, S. J. George, *Adv. Funct. Mater.* **2020**, *30*, 2003693.

RESEARCH ARTICLE

Entry for the Table of Contents



A solid supramolecule based on a sulfobutylether- β -cyclodextrin and diarylethene derivative has been developed by a bromonaphthylpyridinium polymerization strategy. The supramolecule exhibits tunable phosphorescence emission in the amorphous state and can be applied for stimuli-responsive data encryption and anti-counterfeiting.